Mixed region collapse with internal wave generation in a density-stratified medium

By JIN WU

HYDRONAUTICS, Incorporated, Laurel, Maryland

An experiment has been conducted modelling a two-dimensional mixed region collapsing in a continuously density-stratified medium. The process of collapse can be divided into three stages. Empirical formulae have been derived to describe the process of the first two stages, during which gravitational effects determine the modelling criterion. The collapse in the final stage is complicated by viscous effects; a ratio between the Froude number and the Reynolds number seems to provide a probable modification of the time scale.

The pattern of internal waves generated by the initial impulsive collapse of this mixed region can be represented by moving rays connecting either wave crests or troughs. These rays move away from the collapse centre and at the same time decrease their slopes from the horizontal. A simpler steady-state wave pattern generated by an oscillating plunger has also been studied. Taken together, these experimental results are interpreted to show that the energy density of the collapse is skewed toward high frequencies and is peaked at $\frac{8}{10}$ of the Brunt–Väisälä frequency of the medium.

1. Introduction

It is well known that a stable density stratification generally exists in the ocean and the atmosphere. The present study concerns a mixed region formed in such a medium by a disturbance; submarine wakes in the ocean and contrails in the atmosphere are notable examples. This mixed region may also be formed at the crests of large amplitude waves, such as lee waves in air streams over a mountain and internal waves in the ocean. The experiments have been conducted for the sake of simplicity with a linear density gradient, which adequately for our purpose approximates the stable density stratifications in nature.

The wake generated by a submerged body moving through a density-stratified medium is a region of turbulent, mixed fluid with homogeneous density. Due to the stabilizing effect of the stratification, turbulence near the wake boundary is rapidly damped, and does not cause appreciable mixing of the mixed fluid with its surroundings. Therefore, as the mixed fluid seeks to return to its equivalent density level, the region collapses vertically—first demonstrated by Schooley & Stewart (1963), and internal waves are consequently generated. Because the wake is very slender in the direction of body passage, vertical collapse and the genera-

tion of internal waves can be effectively and adequately studied by means of a two-dimensional, initially circular, non-turbulent mixed region.

The purposes of the present research are to study experimentally the modelling criteria relating to the collapse of such a region, to determine the characteristic frequency of collapse and the pattern of internal waves subsequently generated.
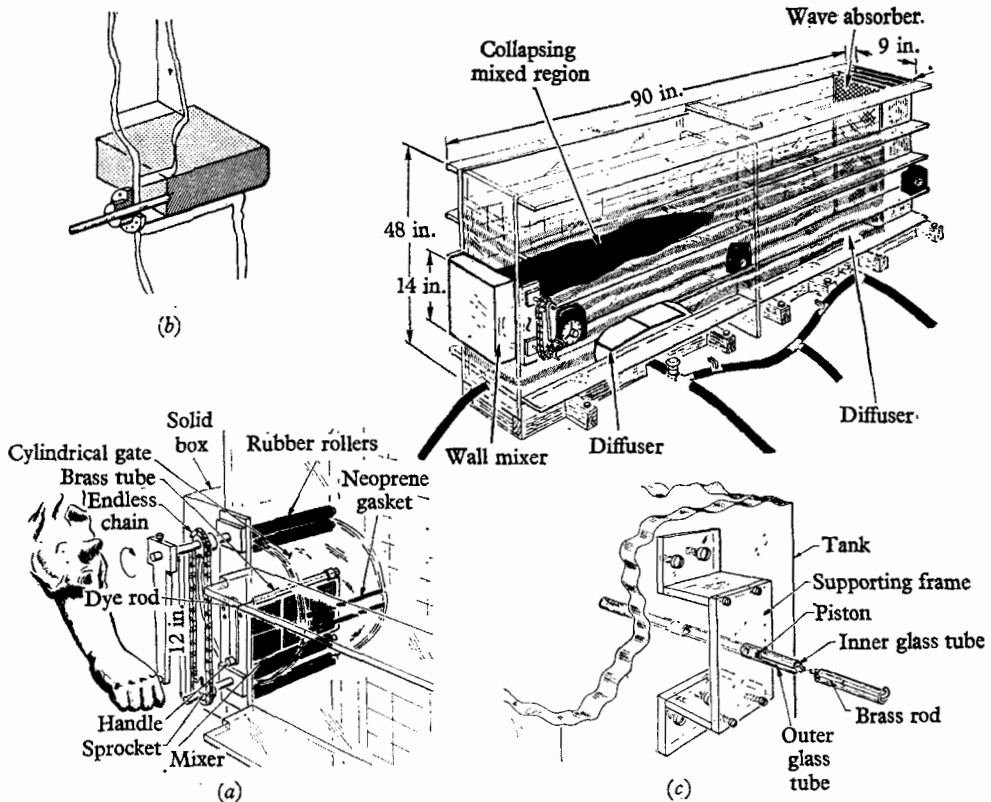

FIGURE 1. General view of equipment. (*a*) Wall mixer and controlling device. (*b*) Oscillating plunger, replacement of wall mixer. (*c*) Fluid sampling device.

2. Equipment and experimental procedures

The experiment is conducted in a transparent tank, see figure 1. Layers of fluid with increasing densities (increasing salt concentration in water) are introduced successively through diffusers at the tank bottom. The layers are 1 in. thick, with every other one coloured by red dye. Overnight, the fluid acquires through molecular diffusion a linear density stratification from the initial step-distribution. This linear stratification has been verified by determining the density of the fluid sampled from the tank. Care is taken to withdraw the entire sample from the same density level. As shown in figure 1 (*c*), a brass rod with a piston at one end is placed inside the inner glass tube, and the other end of the rod is bent and hooked to the far end of the outer glass tube. As the inner tube, supported horizontally by a frame, is slowly inserted into the tank, the outer tube is stopped by the frame. The brass rod, held by the outer tube, thus in turn holds the piston at rest.

The fluid which has filled the space now occupied by the glass tube is then drawn into the tube. Samples from different layers can be withdrawn by either draining fluid from or introducing fluid into the tank through the diffusers.

Since the molecular diffusion rate of dye is much smaller than that of salt, even after the linear density gradient has been obtained in the fluid, the boundaries of the red layers (which are isopycnic lines) remain distinctly visible. This fact is crucial for the observation of internal waves.

A 'wall mixer' is installed at the upstream end of the tank to generate a two-dimensional, semi-circular mixed region; see figure 1 (*a*). Two thin circular cylindrical pieces, 110° sectors with a diameter of 12 in., are used as the gates. These transverse cylindrical gates are fitted tightly between two pairs of rubber rollers placed separately in two slots opened in the end wall of the tank. With their shafts connected by a chain, the rollers can be turned synchronously to control the gates. A solid box with a track for the retracted gates is attached to the end wall of the tank. The gates are closed just prior to a test to partition off the stratified fluid for mixing; mixing begins following the insertion of a blue dye rod and is continued until the entrapped fluid achieves a homogeneous (blue) colour, an indication of uniform density. This density should be the same as that of the surrounding fluid at the centre of the mixed region. The mixed fluid is then left inside the gates to wait for the turbulence to be sufficiently damped before releasing it. The boundary layers along the gates, which can be opened within $\frac{8}{10}$ sec, have no chance to develop and no appreciable secondary flow seems to be introduced. This has been checked by applying the same technique in pure water. In this case, after the gates have opened, the blue-coloured water diffuses very slowly outward while keeping its semicircular shape.

Further, in order to understand more about the internal wave pattern generated by the collapse, steady-state waves have been studied in an experiment where the wall mixer is replaced by an oscillating plunger (a two-dimensional pulsating disturbance). The plunger, as shown in figure 1 (*b*), consists of a block, 2 in. thick, and can be driven at any desired frequency.

The collapse (the motion of the uniform density, blue-coloured mixed region inside the linearly stratified medium with alternately red-coloured layers) and the internal wave pattern (undulations of the red layers) are photographed with a movie camera.

Ten tests with density stratifications ranging between $a = -(1/\rho_0)\,\partial\rho/\partial y = 0.002$ and 0.092 ft.$^{-1}$ have been conducted with the wall mixer; see figure 10, plate 1, for nomenclature. The upper limit of the density gradient is constrained by the solubility of salt in water and the lower limit is restricted by the capability of the fluid-introducing technique. With the oscillating plunger, three tests with density stratifications, $a = 0.006$, 0.023 and 0.062 ft.$^{-1}$, have been performed.

Jin Wu

3. Collapse of a mixed region

3.1. *Width, profiles and areas of the collapsing region*

Profiles of the collapsing region are traced from the film; sample pictures are shown in figure 10 (*a*), plate 1. Since the collapse is believed to be primarily a gravitational flow phenomenon, the dimensionless widths of the collapsing region, x/x_0, where x_0 is the initial width, were first plotted versus the dimensionless time, $t\sqrt{(ag)}$, where g is the gravitational acceleration. The curves have the same general shape shown in figure 2 (*a*), being concave upward for the first part

Density stratification		Lower tangent point		Upper tangent point	
$a = -(1/\rho_0)\,\partial\rho/\partial y$, ft.$^{-1}$		x/x_0	$t\sqrt{(ag)}$	x/x_0	$t\sqrt{(ag)}$
0·0020		2·2	3·1	6·7	17
0·0040		2·1	3·0	6·8	22
0·0081		2·1	3·3	7·2	28
0·0155		2·1	3·2	7·0	24
0·0233		2·1	3·2	6·9	25
0·0310		2·0	3·2	6·3	25
0·0386		2·1	3·2	6·6	25
0·0458		2·0	3·2	6·6	27
0·0807		2·0	3·0	6·2	26
0·0921		2·0	3·1	6·2	21

TABLE 1. Classification of collapse stages

followed by a straight-line segment and then continuing with a concave downward curve. The co-ordinates of the upper and lower tangent points of the straight-line segments are approximately the same for all values of a, and are compiled in table 1.

The profiles of the mixed region during its collapse are observed to follow the same systematic changes shown in figure 2 (*b*). The region shown initially as profile (1) collapses rather suddenly in the beginning. An elevated head, shown as profile (2), is observed to follow the initial impulsive collapse. The elevated parts then cause a secondary collapse: flattening first the elevated parts, profile (3), and then developing a small wedge in front of the region proper, profile (4). Finally, this small wedge is caught up by the region proper and a long, thin triangular wedge is formed, profile (5). The collapse progresses further after this formation, but the shape is unchanged.

Taking together figure 2 (*a*) and table 1, we assume that there are three stages of collapse, 'initial,' 'principal' and 'final' collapse stages, respectively. The region front with the elevated head is observed at $t\sqrt{(ag)} \doteq 3$ and the long, thin triangular wedge is first developed around $t\sqrt{(ag)} \doteq 25$. These two times were found to correspond to the lower and upper tangent points of the middle straight-line segment shown in figure 2 (*a*). In other words, the initial collapse stage ends with the development of profile (2), the principal stage ends with profile (5), then the final stage ensues.

Further discussion of the collapse process will be presented in the next section. At this point, it may be worthwhile to show that the fluid inside the region closely maintains its density during the entire process of collapse.

The velocity and density gradients at the interface separating stationary fresh water and under-flowing salt water were reported by Lofquist (1960). In addition, re-examining Lofquist's data, we find that the maximum velocity of the salt
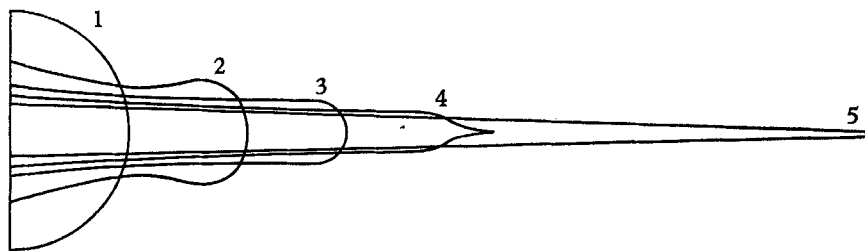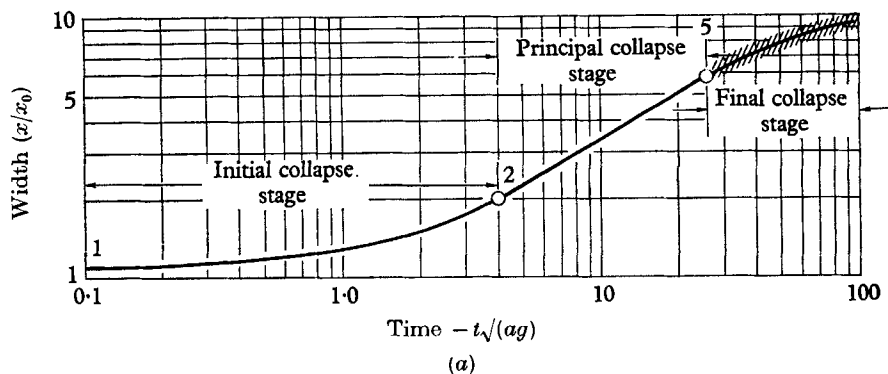

(a)

(b)

FIGURE 2. Stages and profiles of a collapsing mixed region. (*a*) Stages of collapse. (*b*) Profiles of collapse.

water occurs at a distance $h = 1 \cdot 25 h_r$ below the interface, where h_r is the hydraulic radius. The Richardson number, R_i, at the interface can be written as

$$R_i = \frac{-\dfrac{g}{\rho}\left(\dfrac{\partial \rho}{\partial y}\right)_{if}}{\left(\dfrac{\partial u}{\partial y}\right)_{if}^2} = 0 \cdot 58 \left(\frac{\Delta\rho}{\rho}\right)\left(\frac{\bar{\nu}}{\nu_s}\right)^2\left(\frac{\bar{u}}{u_0}\right)^2\left(\frac{gh}{u_0^2}\right), \tag{1}$$

where ρ, ν_s, $\bar{u}$ and u_0 are the density, kinematic viscosity, average and maximum velocities of the salt water, respectively; $\Delta\rho$ is the density jump at the interface; $\bar{\nu}$ is the average kinematic viscosity of the salt and fresh water.

Two abrupt density jumps similar to that at the fresh and salt water interface occur at the top and bottom boundaries of the mixed region; see figure 10 (*a*). If (1) is applied to this case, h can be taken as the half-thickness of the region,

$\frac{1}{2}y_w$, ν and ν_s can both be taken as that of the stratified fluid at the elevation of the region centre; we now have,

$$R_i = 0{\cdot}23 \left(\frac{y_w}{x_0}\right)^2 \left(\frac{\bar{u}}{u_0}\right)^2 \left(\frac{\sqrt{(ag)}x_0}{u_0}\right)^2. \tag{2}$$

By assuming $\bar{u} = 0{\cdot}85u_0$, the Richardson numbers at the top and bottom boundaries of the mixed region, found from (2), are always greater than $\frac{1}{2}$. However, $R_i = \frac{1}{4}$ is the criterion for stability beyond which no turbulence is likely to be generated (Schlichting 1958).
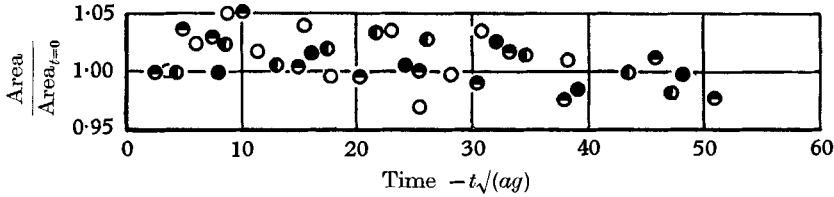

FIGURE 3. Areas of a collapsing mixed region. The areas are determined from the traced region profiles with the aid of a planimeter. The different symbols represent results from different tests: $\bigcirc$, $a = 0{\cdot}0020$ ft.$^{-1}$; $\ominus$, $a = 0{\cdot}0081$ ft.$^{-1}$; $\mathbb{O}$, $a = 0{\cdot}0233$ ft.$^{-1}$; $\bullet$, $a = 0{\cdot}0807$ ft.$^{-1}$.

The observation of a sharp boundary of the mixed region in all tests seems to confirm that no appreciable turbulent mixing takes place (molecular diffusion can be ignored in view of the short test period). Furthermore, the general trend of the areas of the collapsing region, plotted in figure 3, indicates no appreciable volume change during collapse. The data points are scattered because the collapsing region is not exactly two-dimensional.

3.2. *Modelling criterion for collapse of a mixed region*

Froude scaling for initial and principal collapse stages. For the principal stage of collapse, corresponding to the straight line segment shown in figure 2 (*a*), the data from different runs follow closely a collinear trend. In order to investigate the initial stage further, corresponding to the concave upward curve in figure 2 (*a*), the results were plotted differently emphasizing the initial collapse, adopting $(x - x_0)/x_0$ rather than x/x_0. It was found that this part of the experimental data also follows a collinear trend.

In summary, the collapse process during the initial and principal stages can be expressed, respectively, as

$$(x - x_0)/x_0 = c(t\sqrt{(ag)})^m; \quad x/x_0 = c(t\sqrt{(ag)})^m. \tag{3}$$

The rate of collapse, V, can thus be written as,

$$\frac{V}{\sqrt{(ag)}x_0} = k(t\sqrt{(ag)})^{m-1}, \tag{4}$$

where c, m and k are numerical constants; the terms $\sqrt{(ag)}x_0$ and $1/\sqrt{(ag)}$ are characteristic velocity and time, respectively, defined for a continuously density-stratified medium. The values of c and m, averaged from ten runs with different

density stratifications, are compiled in table 2. The maximum deviations of the original values from their averages are shown in parentheses. The values of k are determined from the average values of c and m.

It is clear from (3) that the collapse during the initial and principal stages is primarily a gravitational flow phenomenon, and that the collapse process during these stages is identical for all tests with different density stratifications if we observe them on the basis of a transformed time scale, $t\sqrt{(ag)}$. The left-side of (4)

Collapse stages	Experimentally determined constants				Ranges of applicability	
	c	m	k	$m - 1$	x/x_0	$t\sqrt{(ag)}$
Initial	0·29 (0·04)	1·08 (0·05)	0·32	0·08	1–1·75	0–2·5
Principal	1·03 (0·05)	0·55 (0·02)	0·57	− 0·45	2–6·75	3–25

TABLE 2. Initial and principal stages of collapse

is essentially a densimetric Froude number. This number (or the non-dimensional collapse rate) varies with the non-dimensional time $(t\sqrt{(ag)})$ exactly in the same manner for tests with different density stratifications. In other words, the collapse process obeys Froude-number scaling, provided, of course, that no mixing takes place between the wake and its surrounding.

For mixed regions occurring in the field, their physical dimensions, x_0, are greater (by one or two orders of magnitude) than those modelled in the laboratory. However, some density gradients, a, chosen in this study are much greater (by five or six orders of magnitude) than the natural stratification. Consequently, the Reynolds numbers, $\sqrt{(ag)}x_0^2/\nu$, for natural phenomena are believed to be partially represented by the present experimental conditions.

Froude and Reynolds scaling for final collapse stage. During the final stage of collapse, the viscous effects become appreciable. This effect is evident from the data which show that runs with lower density gradients and smaller rates of spreading were found to be slowed down faster. It is suggested that the ratio between the Froude and Reynolds numbers

$$\frac{F}{R} = \frac{V/\sqrt{(ag)}\,x_0}{\rho_0\,Vx_0/\bar{\mu}} = \frac{\bar{\mu}}{\rho_0\sqrt{(ag)}\,x_0^2}, \tag{5}$$

denoting the interaction between the gravitational cause of the collapse and the viscous resistance to collapse, may provide a modification factor for the transformed time scale, $t\sqrt{(ag)}$, the inherent scale for the stratified medium.

The data, plotted in figure 4, are scattered, but they are not in contradiction to this suggested modification factor. The data from two tests with the lowest density gradient deviate far from the others, since mixing at the thin tip of the mixed region was observed during these two tests.
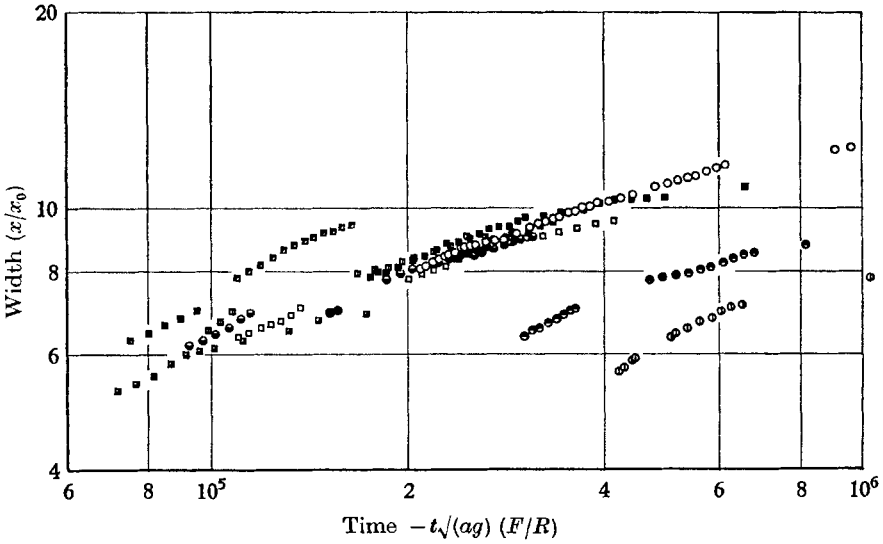
FIGURE 4. Final stage of collapse. $\oslash$, $A = 0.0020$ ft.$^{-1}$; $\ominus$, $A = 0.0040$ ft.$^{-1}$; $\bigcirc$, $A = 0.0081$ ft.$^{-1}$; $\bullet$, $A = 0.0155$ ft.$^{-1}$; $\blacksquare$, $A = 0.0233$ ft.$^{-1}$; $\square$, $A = 0.0310$ ft.$^{-1}$; $\boxdot$, $A = 0.0386$ ft.$^{-1}$; $\ominus$, $A = 0.0458$ ft.$^{-1}$; $\boxslash$, $A = 0.0807$ ft.$^{-1}$; $\boxslash$, $A = 0.0921$ ft.$^{-1}$.

$$a = -\frac{1}{\rho_0}\frac{\partial\rho}{\partial y} = 0.0233 \text{ ft.}^{-1}$$

Definition sketch
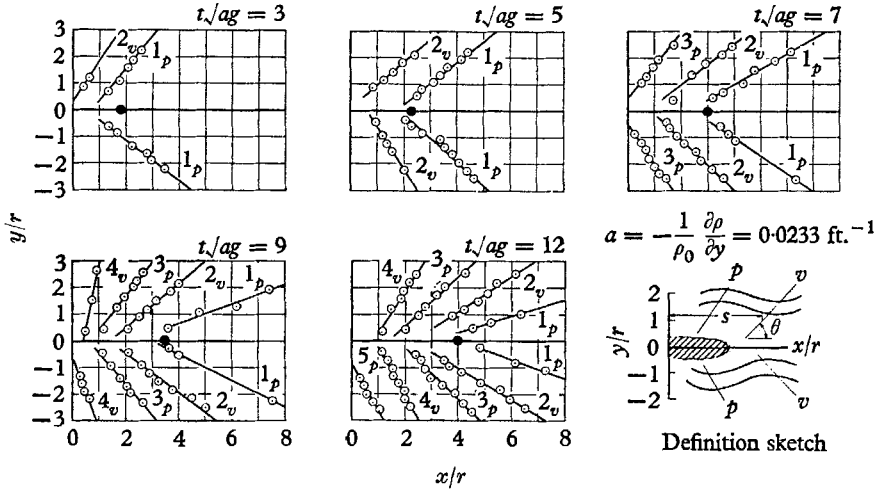
FIGURE 5. General pattern of internal waves generated by a collapsing mixed region. The waves, $\odot$, are seen to pass the front of the collapsing region, $\bullet$, gradually since the rate of collaps‡ slows down continuously while each crest or trough was observed to propagate downstream along the isopycnic line with a nearly constant velocity.

4. Pattern of internal waves

During the initial impulsive collapse of the mixed region, the fluid layers near the collapsing centre displace continuously toward the centre along two inclined narrow zones (see sample pictures shown in figure 10 (a)) and reach their maximum deflexions at the end of the initial collapse stage. As the deflected layers oscillate back toward their equilibrium positions, undulations of the isopycnic lines are observed. Shown by locations of the crests (p) and troughs (v) of the undulation, a sample wave pattern is presented in figure 5, in which r is the radius of the initial mixed region. As shown in figure 5, the trace of the crests or troughs at various elevations can be connected by a straight line. The order of wave generation is indicated by number, and the subscript distinguishes crest from trough. These straight lines, like rays, are seen to move away from the collapse centre and at the same time decrease their slopes from the horizontal. Three tests with the 'wall mixer' technique have been chosen for studying the internal wave pattern; based on a transformed time scale, $t\sqrt{(ag)}$, an identical wave pattern is observed for two other runs with different density stratifications. This means that higher frequency waves propagate in stiffer media exactly according to the variation in the Brunt–Väisälä frequency, defined as $N = \sqrt{(ag)}$. This pattern is subsequently distorted presumably due to multiple wave generation and reflexions from the tank wall and the free surface. (As discussed later, the wake collapse has a band of frequencies associated with it.)

The moving rays, described by their angles of inclination (θ), and by their intercepts (s) with $y = \pm r$, compiled from three tests are presented in figure 6. The points are scattered, but no great deviation is seen from the mean line based on the combined data of all three runs. This indicates that these rays pass stations at fixed distances away from the collapse centre with identical slopes. In other words, at each station the path of fluid-particle oscillation is independent of time. This would seem to suggest that the initial impulsive collapse of the mixed region (a punch-type action) is totally responsible for the generation of the internal waves.

A plot concerning the wave heights is not shown here; but, generally speaking, wave heights as large as two-tenths of the mixed-region radius are generated. The maximum wave heights always occur along the two narrow zones where the deflexions of the fluid layers are first seen. While propagating from the collapse centre, all undulations continuously and rather rapidly suffer reductions in their heights. No systematic variation in runs with different density stratifications was observed. In summary, the wave height as well as the wavelength (which can be discerned from figure 5) is characterized by the scale of the mixed region.

In order to understand more about the wave pattern generated by collapse, a steady-state pattern generated by an oscillating plunger was studied; sample pictures are shown in figure 10 (b). The propagation of the internal waves in this case is limited to two narrow zones radiating from the centre of the disturbance. The diamond pattern shown in the picture is due to wave reflexion from the free surface and the tank bottom. The variation of the angle of inclination of the narrow zone (ϕ) with the oscillating frequency of the plunger (f_p) is presented

in figure 7(a). Since the density stratification is linear, no single Brunt–Väisälä frequency can be adopted to characterize this inhomogeneous medium. Consequently, two different values of the Brunt–Väisälä frequency are selected for the upper and lower half of the medium, respectively; they are the local values at the middle depth of each half of the medium.
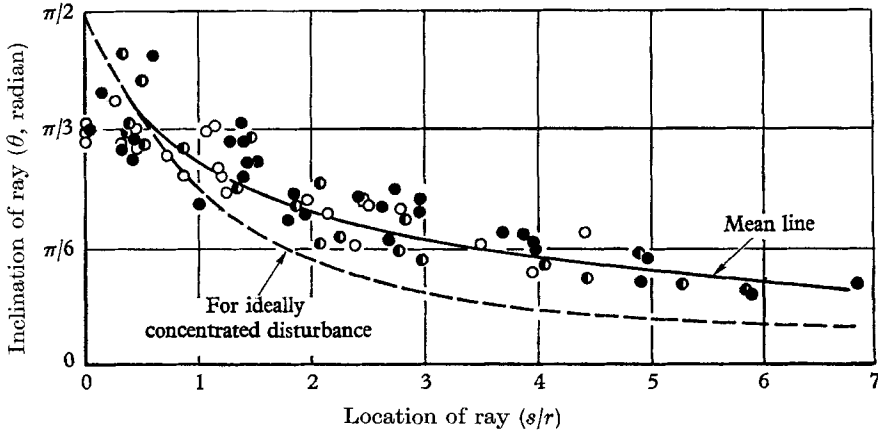

FIGURE 6. Summary of internal wave pattern generated by a collapsing mixed region. The dashed line is a sine curve representing the wave pattern generated by an ideally concentrated disturbance. $\bigcirc$, $N = 0.257$ rad/sec; $\mathbb{O}$, $N = 0.511$ rad/sec; $\bullet$, $N = 0.866$ rad/sec.

The existence of these limited zones (singular lines) and their variations with the frequency of an oscillating disturbance was first shown both theoretically and experimentally by Gortler (1943). Recently, Wong (1965) and Mowbray & Rarity (1967) adapted the Love approximation and the group velocity argument to solve the propagation of the internal waves generated by both an oscillating singularity and an instantaneous source in an anisotropic medium. Toepler–Schlieren pictures similar to those of Gortler's were included in the latter study. In the present experiment, however, with a much simpler experimental set-up (accessible to an ordinary laboratory), it seems possible to obtain more directly visible wave propagation than with the Toepler–Schlieren apparatus. Incidentally, the actual observation or movies of internal wave motion associated with the oscillating plunger offer much better visual acuity than the sample prints shown in figure 10 (b). More than the phase configurations, which are the only thing offered by Toepler–Schlieren pictures, the wave amplitudes (for example) can also be derived from the present prints in terms of the displacements of the clearly observable isopycnic lines.

The energy density for an oscillating singularity with constant amplitude and simple harmonic time dependency (modelled by the oscillating plunger) is concentrated around the frequency of the singularity. The energy is propagating in the direction of the group velocity, shown as the single lines; the inclination of this direction from the horizontal was shown by Wong (1965):

$$\phi = \pm \tan^{-1} \left(\frac{N^2}{f_p^2} - 1 \right)^{-\frac{1}{2}}, \tag{6}$$

which is readily simplified to $\phi = \pm \sin^{-1}(f_p/N)$. (7)

Standing waves are possible within the sector enclosed by the singular lines and the vertical axis passing through the centre of disturbance. Progressive waves are present in the other sector, but do not generally carry enough energy to manifest themselves. The finite width of the singular region shown in the sample
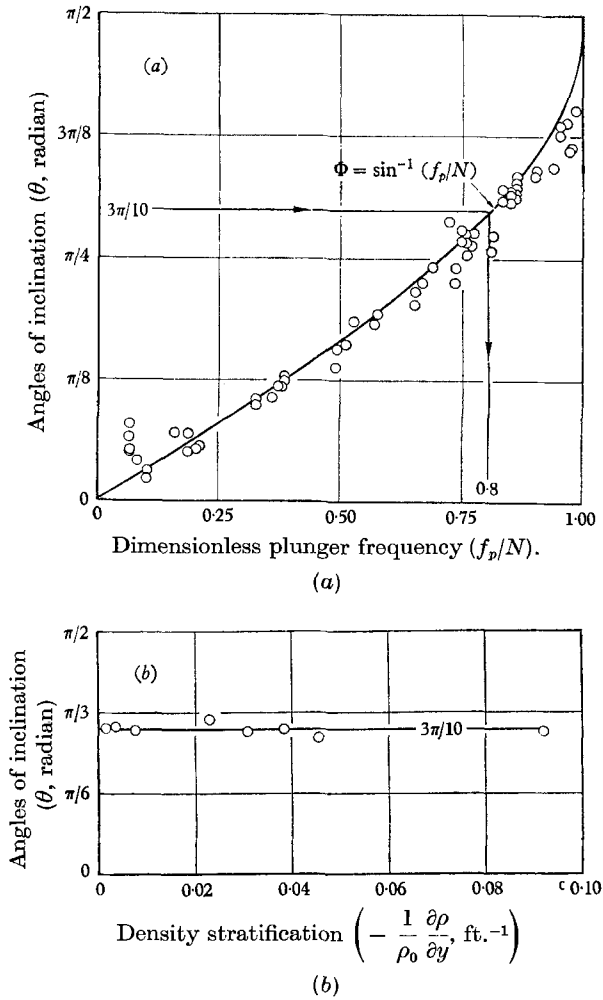

(a)

(b)

FIGURE 7. Comparison of internal waves generated by oscillating plunger and collapsing mixed region. (a) Oscillating plunger. (b) Collapsing region.

pictures is related to the nature of the disturbance (the stroke length of the plunger is 2 in.).

Now let us refer back to the internal waves generated by the collapse of the mixed region. They are not restricted inside the narrow zones. This indicates that, as expected, the energy density of the initial collapse is spread over a wide band of frequencies. On the other hand, as discussed previously, the internal waves are first seen along two narrow zones, in which the maximum wave amplitudes

are also observed. These facts suggest that the energy density associated with the collapse is peaked at some particular frequency. The inclinations of these zones, plotted in figure 7 (b), are seen to be independent of density stratifications and have a value of $3\pi/10$. Corresponding to this angle only, a distinct diamond pattern
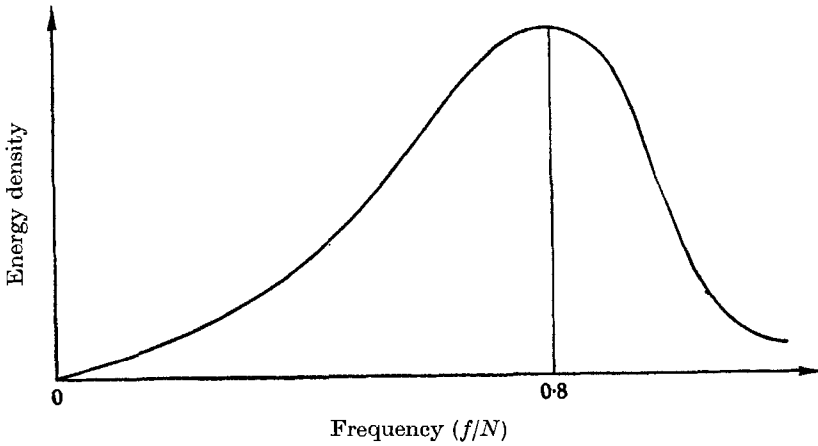

FIGURE 8. Energy density distribution of collapse.

C_g = Group velocity
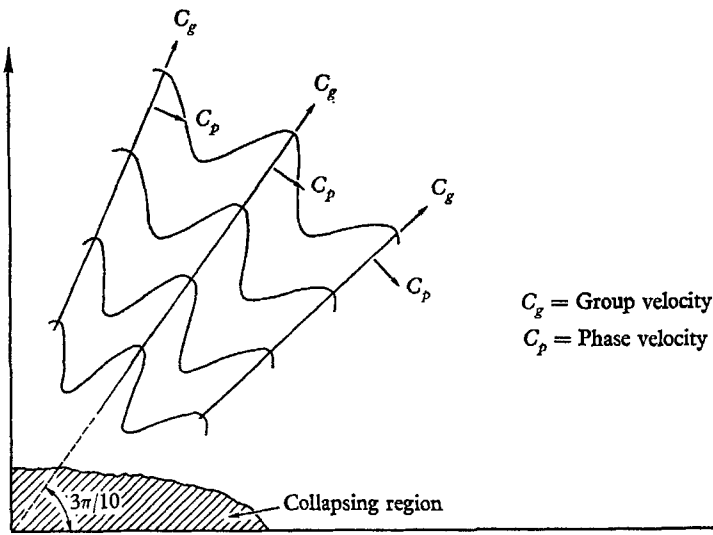C_p = Phase velocity

FIGURE 9. Pattern of internal waves generated by initial impulsive disturbance.

of internal waves generated by the collapse, similar to those shown in figure 10 (b), is observed. Taking these results together, it is found that, around $\frac{8}{10}$ of the Brunt–Väisälä frequency, the energy density of the collapse seems to be peaked. In addition, the smaller amplitude waves observed on the upstream side of these narrow zones, the comparatively larger amplitude waves observed on the down-stream side, and the fact that internal waves with frequencies larger than the Brunt–Väisälä frequency cannot exist, seem further to suggest a skewed energy

density distribution with a slow rising on the low frequency side and a fast dropping at the high frequency side, sketched intuitively in figure 8.

For every frequency, or along any particular ray radiating from the disturbance, internal waves of all wavelengths are possible (Wong 1965); these differ greatly from surface gravity waves, for which a frequency corresponds to only a specific wavelength. However, longer waves move away from the disturbance faster than the short ones. For surface gravity waves, the direction of the wave propagation (phase velocity) coincides with that of the energy propagation (group velocity), but these directions are orthogonal for short internal waves (Lighthill 1960); see figure 9. Since the longer waves have greater phase velocities, the resultant pattern shows that the rays connecting either wave crests or troughs decrease their slopes as they move away from the disturbance. The pattern of the waves is also complicated by the nature of the collapse, which is of course not entirely concentrated at the origin. Further study is needed in order to understand how the match between the energy carrying group velocity and the observed phase velocities, and the adjustment necessary to maintain the observed wave pattern, is brought about.

5. Conclusions

An experiment has been conducted, using a wall-mixer to model the collapse of a non-turbulent mixed region and the subsequent generation of internal waves in a continuously density-stratified medium. The process of collapse can be divided into initial, principal and final collapse stages. For the first two stages, the Froude number is found to be the modelling criterion; empirical formulae have been derived to describe the collapsing process. Based on a transformed time scale, $t\sqrt{(ag)}$, all tests with different density gradients are observed with an identical collapse process. A nearly constant rate of collapse is found for the initial stage, during which the density-stratified layers outside the wake are observed to deform continuously. These deformations start to propagate outward at the beginning of the principal collapse stage; at the same time, the rate of wake collapse slows down gradually. For the final stage, the collapse slows down even further with increasing viscous effects and the collapsing process may be scaled by modifying the transformed time scale with the ratio between the Froude and the Reynolds numbers. The present experimental conditions are believed to include Froude and Reynolds numbers for mixed regions occurring in nature.

The pattern of internal waves generated by the initial impulsive collapse of the mixed region, similar for various density stratifications, can be represented by moving rays connecting either wave crests or troughs. These rays move away from the collapse centre and at the same time decrease their slopes. For further understanding of this complicated transient pattern, a much simpler steady-state case generated by an oscillating plunger is studied. Singular narrow regions, along which the energy of internal waves propagates are clearly observed. In the light of these results, a skewed energy density distribution of the initial impulsive collapse, peaked at $\frac{8}{10}$ of the Brunt–Väisälä frequency, can be deduced. The collapsing wake, mostly due to the initial impulsive collapse, is thus a very

efficient generator of internal waves. In addition, the mechanism of the moving rays and the change of their slopes with locations is partially explained.

REFERENCES

GORTLER, H. 1943 Über eine Schwingungsercheinung in Flüssigkeiten mit stabiler Dichteschichtung. *Z. angew. Math. Mech.* **23**, 65.

LIGHTHILL, M. J. 1960 Studies on magneto-hydromagnetic waves and other anisotropic wave motions. *Trans. Roy. Soc.* A **252**, 397.

LOFQUIST, K. 1960 Flow and stress near an interface between stratified liquids. *Phys. Fluids*, **3**, 158.

MOWBRAY, D. E. & RARITY, S. H. 1967 A theoretical and experimental investigation of the phase configuration of internal waves of small amplitude in a density stratified liquid. *J. Fluid Mech.* **28**, 1.

SCHLICHTING, H. 1958 *Boundary Layer Theory*. New York: McGraw-Hill.

SCHOOLEY, A. H. & STEWART, R. W. 1963 Experiments with a self-propelled body submerged in a fluid with a vertical density gradient. *J. Fluid Mech.* **15**, 83.

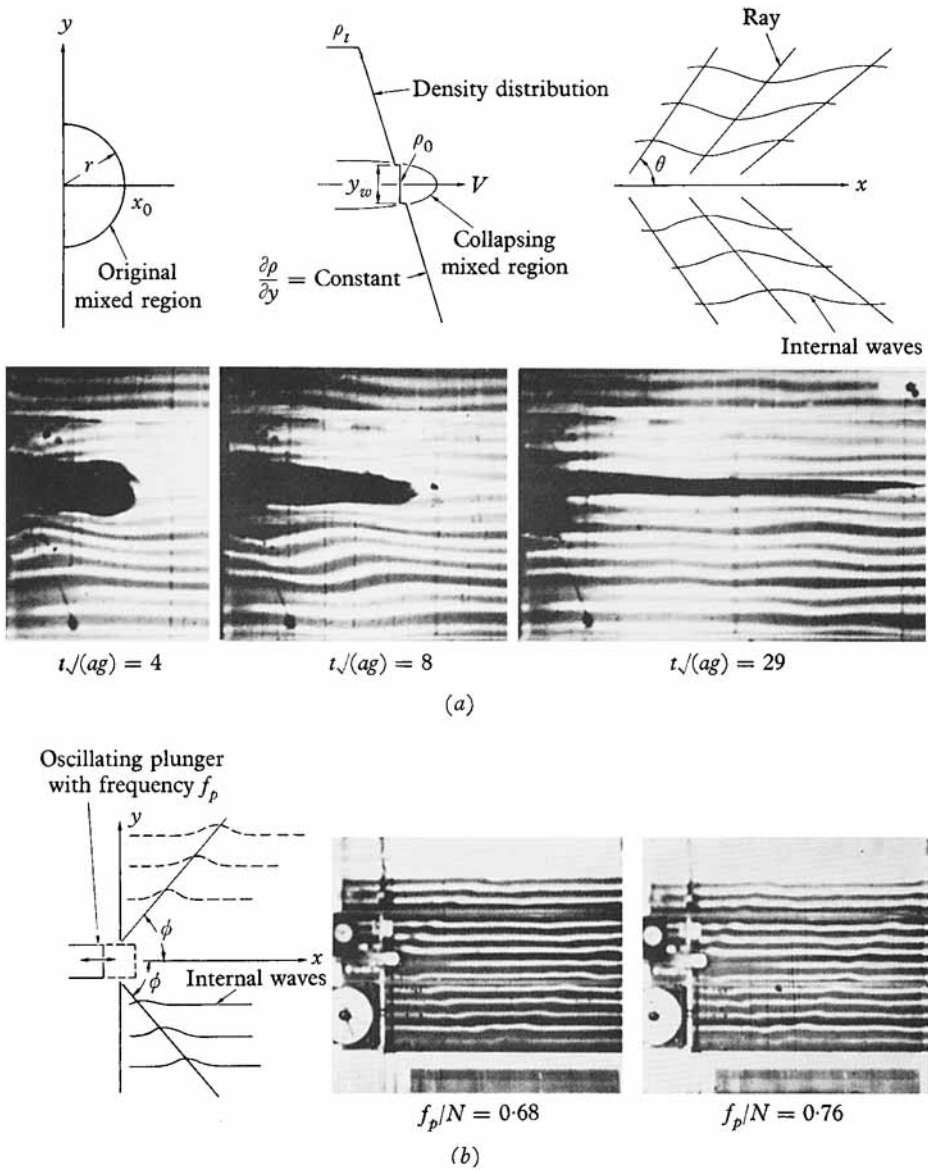WONG, K. K. 1965 On internal gravity waves generated by local disturbance. *Hydronautics, Inc. Tech. Rep.* 231-5.

FIGURE 10. Nomenclature and sample pictures. (a) Collapse of a mixed region and subsequent generation of internal waves. (b) Internal wave generated by an oscillating plunger.